eLIFE elifesciences.org

RESEARCH ARTICLE

Systems analysis of the CO_2 concentrating mechanism in cyanobacteria

Niall M Mangan†*, Michael P Brenner*

School of Engineering and Applied Sciences and Kavli Institute for Bionano Science and Technology, Harvard University, Cambridge, United States

Abstract Cyanobacteria are photosynthetic bacteria with a unique CO_2 concentrating mechanism (CCM), enhancing carbon fixation. Understanding the CCM requires a systems level perspective of how molecular components work together to enhance CO_2 fixation. We present a mathematical model of the cyanobacterial CCM, giving the parameter regime (expression levels, catalytic rates, permeability of carboxysome shell) for efficient carbon fixation. Efficiency requires saturating the RuBisCO reaction, staying below saturation for carbonic anhydrase, and avoiding wasteful oxygenation reactions. We find selectivity at the carboxysome shell is not necessary; there is an optimal non-specific carboxysome shell permeability. We compare the efficacy of facilitated CO_2 uptake, CO_2 scavenging, and HCO_3^- transport with varying external pH. At the optimal carboxysome permeability, contributions from CO_2 scavenging at the cell membrane are small. We examine the cumulative benefits of CCM spatial organization strategies: enzyme co-localization and compartmentalization.

DOI: 10.7554/eLife.02043.001

***For correspondence:** niallmm@gmail.com (NMM); brenner@seas.harvard.edu (MPB)

Present address: †Mechanical Engineering/LMP, Massachusetts Institute of Technology, Cambridge, MA, United States

Competing interests: The authors declare that no competing interests exist.

Funding: See page 14

Received: 11 December 2013
Accepted: 12 April 2014
Published: 29 April 2014

Reviewing editor: Ron Milo, Weizmann Institute for Science, Israel

Introduction

Intracellular compartments are critical for directing and protecting biochemical reactions. One of the simplest and most striking known examples of compartmentalization are the carboxysomes (***Cannon et al., 2001***; ***Yeates et al., 2008***) of cyanobacteria and other autotrophic proteobacteria (***Savage et al., 2010***; ***Rosgaard et al., 2012***). These small, 100−200 nm compartments separate the principal reaction of the Calvin cycle, the RuBisCO catalyzed fixation of carbon dioxide (CO_2) into 3-phosphoglycerate, from the rest of the cell (***Cannon et al., 1991***). CO_2 and oxygen (O_2) competitively bind as substrates of RuBisCO, and the reaction with O_2 produces phosphoglycolate, a waste product which must be recycled by the cell (***Jordan and Ogren, 1981***; ***Tcherkez et al., 2006***; ***Savir et al., 2010***). To maximize carboxylation and minimize oxygenation, the carboxysome is believed to act as a diffusion barrier to CO_2 (***Reinhold et al., 1989***; ***Dou et al., 2008***). There is much interest in the design and function of such compartments and whether they can be used to enhance carbon fixation in other organisms such as plants or to improve reaction rates in other metabolic systems (***Papapostolou and Howorka, 2009***; ***Agapakis et al., 2012***; ***Ducat and Silver, 2012***; ***Frank et al., 2013***). Increased efficiency of biochemical reactions will lead to better yield in bioengineered bacterial systems, creating new possibilities for production of high-value products such as biofuels. Enhancing carbon fixation in plants or other organisms could lead to increased carbon sequestration, or crop yield.

The concentrating mechanism in cyanobacteria relies on the interaction of a number of well characterized components, as shown in ***Figure 1***, transferring inorganic carbon from outside the cell into cytosol and carboxysomes (***Allen, 1984***; ***Kaplan and Reinhold, 1999***; ***Badger and Price, 2003***; ***Price et al., 2007***). Due to this mechanism, inorganic carbon concentration is elevated well above 200–300 μM, the CO_2 concentration required for saturating the RuBisCO. Additionally a high CO_2 concentration increases the ratio of CO_2 to O_2 so that carboxylation dominates over oxygenation. Concentrations of 20–40 mM inorganic carbon, up to 4000-fold higher than external levels, have been observed (***Sultemeyer et al., 1995***; ***Price et al., 1998***; ***Kaplan and Reinhold, 1999***; ***Woodger et al.,***

eLife digest Cyanobacteria are microorganisms that live in water and, like plants, they capture energy from the sun to convert carbon dioxide into sugars and other useful compounds. This process—called photosynthesis—releases oxygen as a by-product. Cyanobacteria were crucial in making the atmosphere of the early Earth habitable for other organisms, and they created the vast carbon-rich deposits that now supply us with fossil fuels. Modern cyanobacteria continue to sustain life on Earth by providing oxygen and food for other organisms, and researchers are trying to bioengineer cyanobacteria to produce alternative, cleaner, fuels.

Understanding how cyanobacteria can be as efficient as possible at harnessing sunlight to 'fix' carbon dioxide into carbon-rich molecules is an important step in this endeavor. Carbon dioxide can readily pass through cell membranes, so instead cyanobacteria accumulate molecules of bicarbonate inside their cells. This molecule is then converted back into carbon dioxide by an enzyme found in specials compartments within cells called carboxysomes. The enzyme that fixes the carbon is also found in the carboxysomes. However, several important details in this process are not fully understood.

Here, Mangan and Brenner further extend a mathematical model of the mechanism that cyanobacteria use to concentrate carbon dioxide in order to explore the factors that optimize carbon fixation by these microorganisms. Carbon fixation is deemed efficient when there is more carbon dioxide in the carboxysome than the carbon-fixing enzyme can immediately use (which also avoids wasteful side-reactions that use oxygen instead of carbon dioxide). However, there should not be too much bicarbonate, otherwise the enzyme that converts it to carbon dioxide is overwhelmed and cannot take advantage of the extra bicarbonate.

Mangan and Brenner's model based the rates that carbon dioxide and bicarbonate could move in and out of the cell, and the rates that the two enzymes work, on previously published experiments. The model varied the location of the enzymes (either free in the cell or inside a carboxysome), and the rate at which carbon dioxide and bicarbonate could diffuse in and out of the carboxysome (the carboxysome's permeability). Mangan and Brenner found that containing the enzymes within a carboxysome increased the concentration of carbon dioxide inside the cell by an order of magnitude. The model also revealed the optimal permeability for the carboxysome outer-shell that would maximize carbon fixation.

In addition to being of interest to researchers working on biofuels, if the model can be adapted to work for plant photosynthesis, it may help efforts to boost crop production to feed the world's growing population.

DOI: 10.7554/eLife.02043.002

2005). The bilipid outer and cell membranes are highly permeable to small uncharged molecules such as CO_2 (***Gutknecht et al., 1977***; ***Missner et al., 2008***), so instead the cell primarily accumulates the charged and less membrane soluble bicarbonate (HCO_3^-) (***Volokita et al., 1984***; ***Price and Badger, 1989***). Active transporters, both constitutive and inducible, bring HCO_3^- into the cell (***Omata et al., 1999***; ***Price et al., 2004***, ***2008***), and mechanisms exist to actively convert CO_2 to HCO_3^- at the thylakoid and cell membrane (***Shibata et al., 2001***; ***Maeda et al., 2002***; ***Price et al., 2008***). Once it passively diffuses into the carboxysome, HCO_3^- is rapidly brought into equilibrium with CO_2 by the enzyme carbonic anhydrase, resulting in the production of CO_2 near RuBisCO. Carbonic anhydrase is known to be localized on the interior side of the carboxysome shell (***Cannon et al., 1991***; ***Cot et al., 2008***; ***Long et al., 2008***; ***Yeates et al., 2008***). The carboxysome shell must be permeable enough to allow HCO_3^- and 3-phosphoglycerate to readily diffuse in and out. The function of this system and its ability to concentrate inorganic carbon depends on the interplay between these various molecular components. Without a model, flux measurements cannot determine the components relative roles in enhancing the CO_2 concentration in the carboxysome. To date, it has not been possible to directly measure the partitioning of the internal carbon concentration in the cytosol and carboxysomes. We wish to characterize the distribution of internal carbon. Visualizations of the location of the carboxysomes with fluorescent microscopy in *S. elongatus* PCC7942 demonstrated that the carboxysomes are evenly spaced along the centerline of the cell, (***Savage et al., 2010***), raising the question of how spatial organization, beyond simple partitioning, changes the efficacy of the system.

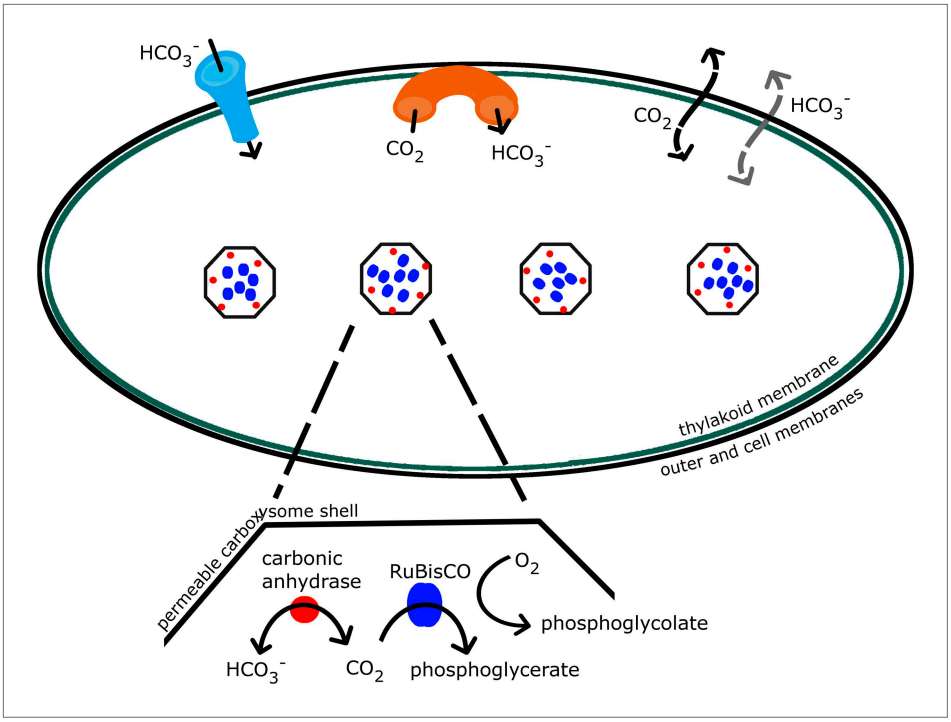

Figure 1. Schematic of the CCM in cyanobacteria. Outer and cell membranes (in black), as well as, thylakoid membranes where the light reactions take place (in green) are treated together. Carboxysomes are shown as four hexagons evenly spaced along the centerline of the cell. The model treats a spherically symmetric cell, with one carboxysome at the center. Active HCO_3^- transport into the cell is indicated (in light blue), as well as active conversion from CO_2 to HCO_3^- at the membranes, sometimes called 'facilitated uptake' or 'scavenging' (in orange). Both CO_2 and HCO_3^- can leak in and out of the cell, with CO_2 leaking out much more readily. Both species passively diffuse across the carboxysome shell. Carbonic anhydrase (red) and RuBisCO (blue) are contained in the carboxysomes and facilitate reactions as shown.

DOI: 10.7554/eLife.02043.003

The goal of this study is to further develop a mathematical model of the CCM (***Reinhold et al., 1989***, ***1991***; ***Fridlyand et al., 1996***) that uses recent experimental progress on the CCM to untangle the relative roles of the different molecular components, and predict the region of parameter space where efficient carbon fixation occurs. We are considering conditions where CO_2 is limiting (15 μM external inorganic carbon) and, for the moment, ignore other biological pressures. In this context, efficient carbon fixation requires two conditions: First, the CO_2 concentration must be high enough that RuBisCO is saturated, and the competitive reaction with O_2 is negligible. We emphasize that for the oxygenation reaction to be negligible the CO_2 concentration should be higher than needed to merely saturate RuBisCO. Secondly, the carbonic anhydrase within the carboxysome must be unsaturated, so that extra energy isn't wasted transporting unused HCO_3^- into the cell.

Examination of the system performance with varying expression levels of HCO_3^- transporters, carboxysome permeability, and conversion from CO_2 to HCO_3^-, reveals a parameter window where these conditions are simultaneously satisfied. We comment on the relation of this window to measured carbon pools, carbon fixation rates, and HCO_3^- transporters. We find that the HCO_3^- concentration in the cytosol is constant across the cell, set by the HCO_3^- transport and leakage rates, and depends very little on the carboxysome permeability. The carboxysome permeability does, however, set how the CO_2 is partitioned between the carboxysome and cytosol. At optimal carboxysome permeability, HCO_3^- diffusion into the carboxysome is fast enough to supply inorganic carbon for fixation, but the rate of CO_2 leakage out of the carboxysome is low. We explore the fluxes from CO_2 facilitated uptake and scavenging with varying ratios of external CO_2 and HCO_3^-. Finally we discuss the proportion the carbon concentration comes from different methods of spatial organization such as co-localization, encapsulation, and spatial location of carboxysomes. Concentration of carbonic anhydrase increases

the maximum rate of reaction for carbonic anhydrase per volume, causing carbonic anhydrase to saturate at a higher level of HCO_3^-, and achieve an order of magnitude higher local CO_2 concentrations. Encapsulation of the reactions in an optimally permeable carboxysome shell achieves another order of magnitude of CO_2 concentration.

Reaction diffusion model

We present our mathematical model, which captures all aspects of the CCM as described above. This model is an expansion of previously developed models (***Reinhold et al., 1989***, ***1991***; ***Fridlyand et al., 1996***). Our three dimensional model of the CCM solves for both the HCO_3^- and CO_2 concentration throughout the a spherical cell. We solve this model numerically and analytically at steady state for three different spatial organizations of carbonic anhydrase and RuBisCO in the cell (Figure 6): enzymes distributed evenly throughout the cell, enzymes localized to the center of the cell but not encapsulated (as they would be on a scaffold), enzymes encapsulated in a carboxysome. We compare the effects of these scenarios in the discussion section, and for now consider a spherical cell of radius R_b = 0.5 μm with a single spherical carboxysome of radius R_c = 50 nm containing RuBisCO and carbonic anhydrase. Numerical computations are carried out with finite difference methods in MATLAB. The details of analytic solutions are given in the ***Supplementary file 1***.

We include the effects of 3D diffusion, active transport and leakage through the cell membrane, and reactions with carbonic anhydrase and RuBisCO. In the carboxysome ($r < R_c$), the equations governing the HCO_3^- and CO_2, here H and C respectively, are

$$\partial_t C = D\nabla^2 C + R_{CA} - R_{Rub} \tag{1}$$

$$\partial_t H = D\nabla^2 H - R_{CA}, \tag{2}$$

where here D is the diffusion constant, and R_{CA} is the carbonic anhydrase reaction, and R_{Rub} is the RuBisCO reaction. The carbonic anhydrase reactions follows reversible Michaelis–Menten kinetics (***Kaplan and Reinhold, 1999***; ***Price et al., 2007***),

$$R_{CA}(H, C) = \frac{V_{ba}K_{ca}H - V_{ca}K_{ba}C}{K_{ba}K_{ca} + K_{ca}H + K_{ba}C}, \tag{3}$$

where V_{ca} and V_{ba} are hydration and dehydration rates, proportional to the local carbonic anhydrase concentration. K_{ca} and K_{ba} are the concentration at which hydration and dehydration are half maximum. The RuBisCO reaction follows Michaelis–Menten kinetics with competitive binding with O_2, $R_{Rub} = V_{max}C/(C + K_m)$, where $K_m = K_m^{'}(1+O/K_i)$. Here V_{max} is the maximum rate of carbon fixation and K_m is the apparent half maximum concentration value, which has been modified to include competitive binding with O_2, O. K_i is the dissociation constant of O_2 with the RuBisCO and $K_m^{'}$ is the half maximum concentration with no O_2 present. RuBisCO also requires ribulose-1,5-bisphosphate, the substrate which CO_2 reacts with to produce 3-phosphoglycolate. Under CO_2 limiting conditions it has been shown that there is sufficient ribulose-1,5-bisphosphate to saturate all RuBisCO active sites, and the reaction rates are independent of ribulose-1,5-bisphosphate concentrations (***Mayo et al., 1989***; ***Whitehead et al., 2014***).

In the cytosol there is no carbonic anhydrase or RuBisCO activity, so $R_{CA} = 0$ and $R_{Rub} = 0$, and there is only diffusion of CO_2 and HCO_3^-. We do not include the natural, but slow, interconversion of CO_2 and HCO_3^- in the cytosol. This assumption is a good one given that the HCO_3^- concentration is known to be held out of equilibrium in the cell (***Volokita et al., 1984***; ***Price and Badger, 1989***). In agreement with this experimental observation, we find that all the other processes effecting the concentration of HCO_3^- in the cytosol happen much faster than the natural interconversion.

Boundary conditions proscribe the inorganic carbon fluxes into the cell and the diffusion across the carboxysome boundary. We treat the inorganic carbon fluxes at cell and thylakoid membranes together. At this cell boundary, there is passive leakage of both CO_2 and HCO_3^-: the velocity of CO_2 across the cell membrane, k_m^C is about 1000-fold higher than that of HCO_3^-, k_m^H, due to the lower permeability of the membrane to charged molecules. To account for active import of HCO_3^-, we combine the total HCO_3^- flux, j_c, from all HCO_3^- transporters. These transporters include BCT1 (encoded by cpm), which is thought to be powered by ATP; and BicA and SbtA which are thought to be

symporters between HCO_3^- and Na^+, driven by the highly controlled electrochemical gradient for Na^+ (**Omata et al., 1999**; **Price et al., 2004**, **2008**). Additionally, there are two complexes NDH-1_3 and NDH-1_4 responsible for converting CO_2 to HCO_3^-. This conversion is thought to either decrease CO_2, creating a gradient across the membranes and 'facilitating uptake' of CO_2, or 'scavenge' CO_2 which has escaped from the carboxysome. These are localized to the thylakoid and possibly the plasma membrane. They have been linked to the photosynthetic linear and cyclic electron transport chain (**Shibata et al., 2001**; **Maeda et al., 2002**; **Price et al., 2008**). It has been proposed that electron transport drives the formation of local alkaline pockets where CO_2 more rapidly converts to HCO_3^-. We simply describe the conversion with a maximal reaction rate α, and concentration of half maximal activity of K_α. Combining these effects, the boundary condition setting diffusive flux of HCO_3^- and CO_2 at the cell membrane is

$$D\partial_r C = -\frac{\alpha C_{cytosol}}{K_\alpha + C_{cytosol}} + k_m^C (C_{out} - C_{cytosol}) \tag{4}$$

$$D\partial_r H = j_c H_{out} + \frac{\alpha C_{cytosol}}{K_\alpha + C_{cytosol}} + k_m^H (H_{out} - H_{cytosol}) \tag{5}$$

where the subscript *cytosol* and *out* indicate we are taking the concentration immediately inside and outside the cell boundary respectively. The diffusion constant times partial derivatives with respect to the radial coordinate, r, define the diffusive flux at the membrane.

The carboxysome shell is composed of proteins with a radius $R_c \approx 50$ nm. As of yet, there have been no direct measurements of the carboxysome permeability to small molecules. Using the carboxysome geometry, we can calculate an upper bound for the diffusive velocity across the carboxysome shell, which is directly related to the carboxysome permeability. Crystal structures (**Yeates et al., 2007**, **2008**; **Cheng et al., 2008**) show the surface has approximately $N_{pores} = 4800$ small pores with radius $r_{pore} \approx 0.35$ nm, and thickness $l = 1.8$ nm. If k_c is the characteristic velocity that small molecules pass through the shell, these numbers imply the upper bound for diffusive transport $k_c < \frac{\pi r_{pore}^2 D}{4\pi R_c^2 l}(N_{pores}) \approx 0.02 \frac{cm}{s}$. This calculation is done by taking the probability that a molecule will encounter a pore on the carboxysome shell $\left(\frac{N_{pores} \times \text{pore surface area}}{\text{carboxysome surface area}}\right)$ and multipling it by the speed a small molecule will diffuse through the length of the pore (D/l). Since it does not take into account any charge effects, which would add an additional energy barrier, it is an upper bound. Although there has been much speculation that the positively charged pores might enhance diffusion of negatively charged HCO_3^- (**Cheng et al., 2008**; **Dou et al., 2008**; **Yeates et al., 2008**), here we explore the simplest assumption, that both HCO_3^- and CO_2 have the same permeability. Namely, the boundary conditions at the carboxysome shell are

$$D\partial_r C = k_c (C_{cytosol} - C_{carboxysome}) \tag{6}$$

$$D\partial_r H = k_c (H_{cytosol} - H_{carboxysome}). \tag{7}$$

We will vary k_c (henceforth called carboxysome permeability, although it is a velocity) within our model and see that there is a range of k_c where the CCM is effective even with k_c identical for CO_2 and HCO_3^-.

Results

Analysis of model: finding functional parameter space

Now that we have defined our model, we wish to find the range of parameters where efficient carbon fixation occurs. In what follows, we fix the enzymatic rates, cell membrane permeability, and diffusion constant as reported in the literature (**Gutknecht et al., 1977**; **Jordan and Ogren, 1981**; **Heinhorst et al., 2006**; **Missner et al., 2008**; **Tables 1 and 2**). Note that full analytic solutions are available in

Table 1. Parameter values chosen for main set of simulations, unless otherwise indicated

Parameter	Definition	Value	Reference
H_{out}	concentration of bicarbonate outside the cell	14 μM*	(**Price et al., 2008**)
C_{out}	concentration of carbon dioxide outside of cell	0.14 μM*	(**Price et al., 2008**)
D	diffusion constant of small molecules, CO_2 and HCO_3^-	$10^{-5}\frac{cm^2}{s}$	(**Fridlyand et al., 1996**)
k_m^C	permeability of cell membrane to CO_2	$0.3\frac{cm}{s}$	(**Gutknecht et al., 1977**; **Missner et al., 2008**)
k_m^H	permeability of cell membrane to CO_2	$3\times10^{-4}\frac{cm}{s}$	(**Gutknecht et al., 1977**; **Missner et al., 2008**)
R_c	radius of carboxysome	5×10^{-6} cm	(**Schmid et al., 2006**; **Cheng et al., 2008**)
R_b	radius of bacteria	5×10^{-5} cm	(**Savage et al., 2010**)
j_c	HCO_3^- transport rate resulting in 30 mM cytosolic HCO_3^- pool	$0.7\frac{cm}{s}$*	calculated
k_c	optimal carboxysome permeability	$6\times10^{-3}\frac{cm}{s}$*	calculated
V_{cell}	cell volume	5.2×10^{-10} μL	calculated
SA_{cell}	cell surface area	3×10^{-8} cm^2	calculated

*these parameters are varied in the text, but these values are used unless noted otherwise.

DOI: 10.7554/eLife.02043.004

Supplementary file 1 sections S3 and S4, so the effect of varying these parameters can be analyzed. We consider the efficacy of the CCM as a function of j_c, the flux of HCO_3^- into the cell, k_c, the carboxysome permeability, and the parameters (α, K_α) governing the CO_2 facilitated uptake mechanism. Both α and j_c can be regulated by the organism and vary depending on environmental conditions, whereas the carboxysome permeability, k_c, is the parameter with the largest uncertainty and debate (***Cannon et al., 2001***; ***Cheng et al., 2008***; ***Yeates et al., 2008***).

For any given pair of k_c and j_c, we ask whether the CO_2 concentrating mechanism is effective, using the criteria of saturating RuBisCO, reducing oxidation reactions, and not increasing the HCO_3^- concentration beyond carbonic anhydrase saturation. Our central result is presented in ***Figure 2***, which shows the range of k_c and j_c where these conditions are met, assuming that there is no facilitated uptake, α = 0.The blue shaded region shows where RuBisCO is unsaturated, and the red shaded region shows where carbonic anhydrase is saturated. There is a crescent shaped region between these regions, where the CCM is effective according to our criteria. In the white region oxygenation

Table 2. Table comparing enzymatic rates (***Sultemeyer et al., 1995***; ***Woodger et al., 2005***; ***Heinhorst et al., 2006***)

Enzyme reaction	active sites	$k_{cut}\left[\frac{1}{s}\right]$	V_{max} in cell $\left[\frac{\mu M}{s}\right]$	V_{max} in carboxysome $\left[\frac{\mu M}{s}\right]$	$K_{1/2}$ [μM]
carbonic anhydrase hydration	80	8×10^4	1.1×10^4	2×10^8	3.2×10^3
carbonic anhydrase dehydration	80	4.6×10^4	9.5×10^4	1.7×10^8	9.3×10^3
RuBisCO carboxylation	2160	26	103	1.7×10^6	270

V_{max} in cell and carboxysome refer to the volumetric reaction rate assuming the enzymes are distributed through cellout the entire cell or only carboxysome. V_{ba} (V_{max} for carbonic anhydrase dehydration) is estimated by assuming K_{eq} = 5 and using parameters found in ***Heinhorst et al. (2006)***. V_{ca} is V_{max} for carbonic anhydrase hydration. Similarly, K_{ba}, and K_{ca} are $K_{1/2}$ for dehydration and hydration respectively.

DOI: 10.7554/eLife.02043.005

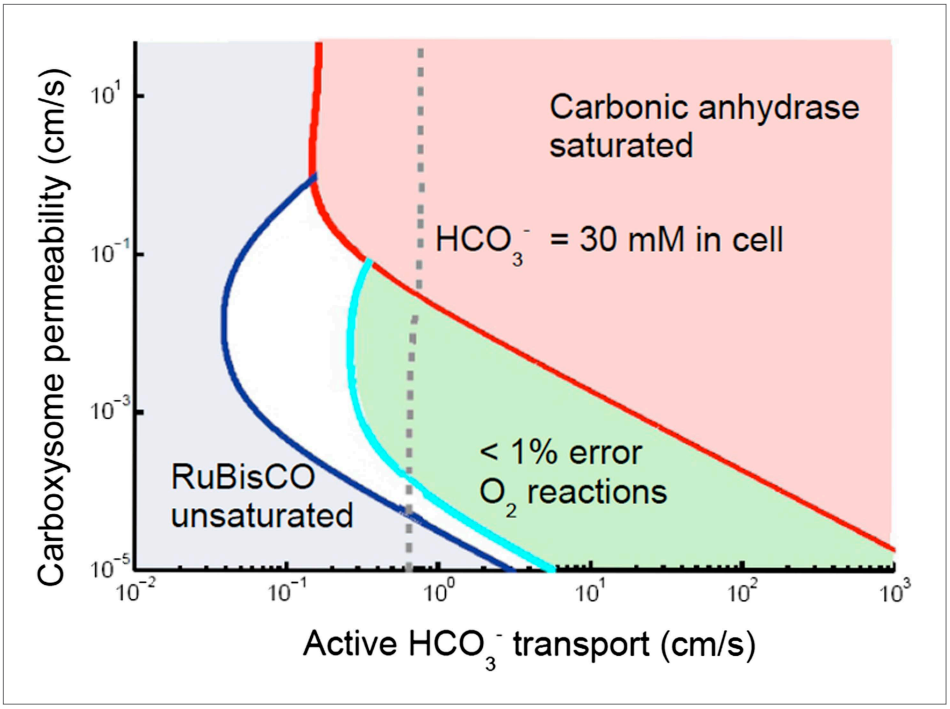

Figure 2. Phase space for HCO_3^- transport, j_c, and carboxysome permeability k_c. Plotted are the parameter values at which the CO_2 concentration reaches some critical value. The left most line (dark blue) indicates for what values of j_c and k_c the CO_2 concentration in the carboxysome would half-saturate RuBisCO (K_m). The middle line (light blue) indicates the parameter values which would result in a CO_2 concentration where 99% of all RuBisCO reactions are carboxylation reactions and only 1% are oxygenation reactions when O_2 concentration is 260 μM. The right most (red) line indicates the parameter values which result in carbonic anyhdrase saturating. Here $\alpha = 0$, so there is no CO_2 scavenging or facilitated uptake. The dotted line (grey) shows the k_c and j_c values, where the HCO_3^- concentration in the cytosol is 30 mM. The HCO_3^- concentration in the cytosol does not vary appreciably with k_c in this parameter regime, and reaches 30 mM at $j_c \approx 0.7 \frac{cm}{s}$. All other parameters, such as reaction rates are held fixed and the value can be found in the ***Table 1 and 2***.

DOI: 10.7554/eLife.02043.006

The following figure supplements are available for figure 2:

Figure supplement 1. Phase space for HCO_3^-transport and carboxysome permeability.

DOI: 10.7554/eLife.02043.007

Figure supplement 2. Effect of CO2 scavenging or facilitated uptake on phase space for HCO_3^-transport, j_c, and carboxysome permeability, K_c.

DOI: 10.7554/eLife.02043.008

reactions happen at a rate of greater than 1%. In the green shaded region oxygenation reactions occur at a rate of less than 1%. Within the white and green regions the CO_2 concentration in the carboxysome varies greatly.

The lines dividing the regions in ***Figure 2*** are lines of constant carboxysomal CO_2 concentration in j_c and k_c parameter space. The dark blue line is where $CO_2 = K_m$, the CO_2 concentration for half maximum RuBisCO reactions. The light blue line indicates parameter values resulting in the CO_2 concentration ($C_{99\%}$) where rate of oxygenation reactions is 1% for O_2 concentration of 260 μM. Varying carboxysome permeability, k_c values, require more or less HCO_3 transport, j_c, to achieve the same carboxysomal CO_2 concentration.

We can calculate an amplification factor for the $C_{99\%}$ line of constant carboxysomal CO_2 concentration as $A_C = \frac{C_{carboxysome}}{C_{out} + H_{out}} = 133$. Any combination of j_c and k_c which produce $C = C_{99\%}$, make 133 times more CO_2 available in the carboxysome than there is total inorganic carbon outside the cell. Generally, increasing HCO_3^- transport, below the carbonic anhydrase saturation point results in higher CO_2 concentration in the carboxysome.

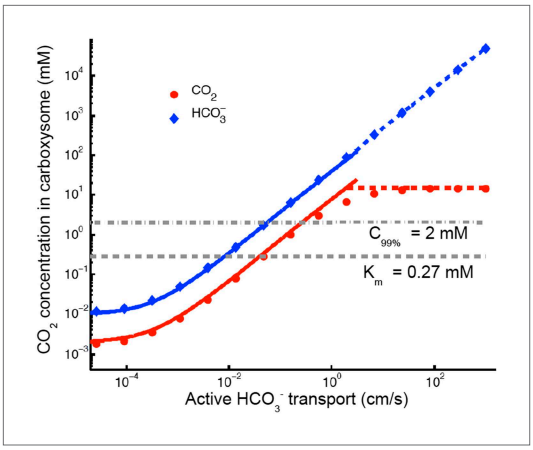

Figure 3. Numerical solution (diamonds and circles) and analytic solutions (carbonic anhydrase unsaturated, solid lines, and saturated, dashed lines) correspond well. HCO_3^- transport is varied, and all other system parameters are held constant. The CO_2 concentration above which RuBisCO is saturated is K_m (grey dashed line). The CO_2 concentration where the oxygen reaction error rate will be 1% is $C_{99\%}$ (grey dash-dotted line). The transition between carbonic anyhdrase being unsatruated and saturated happens where the two analytic solutions meet (where the dashed and solid red lines meet). Below a critical value of transport, $j_c \approx 1e^{-3}\frac{cm}{s}$ the level of transport is lower than the HCO_3^- leaking through the cell membrane.

DOI: 10.7554/eLife.02043.009

The following figure supplements are available for figure 3:

Figure supplement 1. No effect of localizing carbonic anhydrase to the shell of the carboxysome.

DOI: 10.7554/eLife.02043.010

Varying HCO_3^- transport saturates enzymes

The basic physics of the phase diagram ***Figure 2*** follows from examining how CO_2 and HCO_3^- in the carboxysome change as j_c is varied. ***Figure 3*** shows the response to varying j_c, with $k_c = 6 \times 10^{-3}\frac{cm}{s}$ (the optimal value in Figure 4).

When j_c is low, the ratio of CO_2 and HCO_3^- is constant, set by the chemical equilibrium at a given pH. In this case the rate of the carbonic anhydrase reaction is much faster than diffusion within the carboxysome, so that $V_{ba}K_{ca}H = V_{ca}K_{ba}C$. Unlike the uncatalyzed interconversion of CO_2 and HCO_3^- in the cytosol, carbonic anhydrase brings the concentrations in the carboxysome to equilibrium very quickly. The chemical equilibrium is $K_{eq} = H/C = (K_{ba}V_{ca})(K_{ca}V_{ba}) \approx 5$, for pH around 7 (***DeVoe and Kistiakowsky, 1961***), so that $HCO_3^- > CO_2$ in the carboxysome. Increased pH would increase K_{eq} and the proportion of HCO_3^-, while decreased pH would decrease K_{eq} and the proportion of HCO_3^-. Such variations do not substantially effect the subsequent discussion and mechanisms, although they will change the absolute values of CO_2 concentration in the carboxysome.

The K_m dashed line in ***Figure 3*** shows the CO_2 level above which RuBisCO reaction is saturated: this gives the RuBisCO saturated (blue) boundary in ***Figure 2***. We have similarly marked the concentration $C_{99\%}$ where there is a 1% oxygen reaction error rate with a dash-doted line.

At higher levels, the CO_2 concentration no longer increases with increasing j_c, because the carbonic anhydrase is saturated. The saturated regime occurs in ***Figure 3*** when $H_{carboxysome} > K_{ba}$, so that increasing $H_{carboxysome}$ (controlled directly by j_c) no longer increases the rate of production of $C_{carboxysome}$. This transition from unsaturated to saturated carbonic anhydrase defines the line for the carbonic anhydrase saturated region in ***Figure 2***.

Carboxysome permeability has optimal value

For each line of constant concentration in ***Figure 2*** there is an optimal permeability value, where the least HCO_3^- transport is required to achieve the same CO_2 concentration. The optimal permeability value shifts downward with increasing CO_2 concentration (compare light and dark blue curves). For $C_{99\%}$ the optimal permeability is $k_c = 6 \times 10^{-3}\frac{cm}{s}$, below the calculated upper bound: $k_c < 0.02\frac{cm}{s}$ obtained above from the carboxysome structure. To further understand the effect of permeability, we examine the CO_2 concentration in the carboxysome for varying carboxysome permeabilities and a fixed HCO_3^- transport rate in ***Figure 4***. ***Figure 4A***, shows that there is a broad range of k_c where the CCM has maximal efficacy. ***Figure 4*** shows the distribution of inorganic carbon throughout the cell when the permeability is low (B), optimal (C), and high (D). At high permeability, the CO_2 produced in the carboxysome rapidly leaks out of the carboxysome, and the CO_2 concentration in the cytosol, shown in ***Figure 4D***, is relatively high. When the carboxysome permeability decreases to near the optimal value, ***Figure 4D***, the carboxysome traps CO_2, and the cytosolic levels are lower, decreasing leakage out of the cell. This transition occurs when diffusion across the cell (and carboxysome) takes a shorter time than diffusion through the carboxysome shell; or the CO_2 in the carboxysome is effectively partitioned from the CO_2 in the cell.

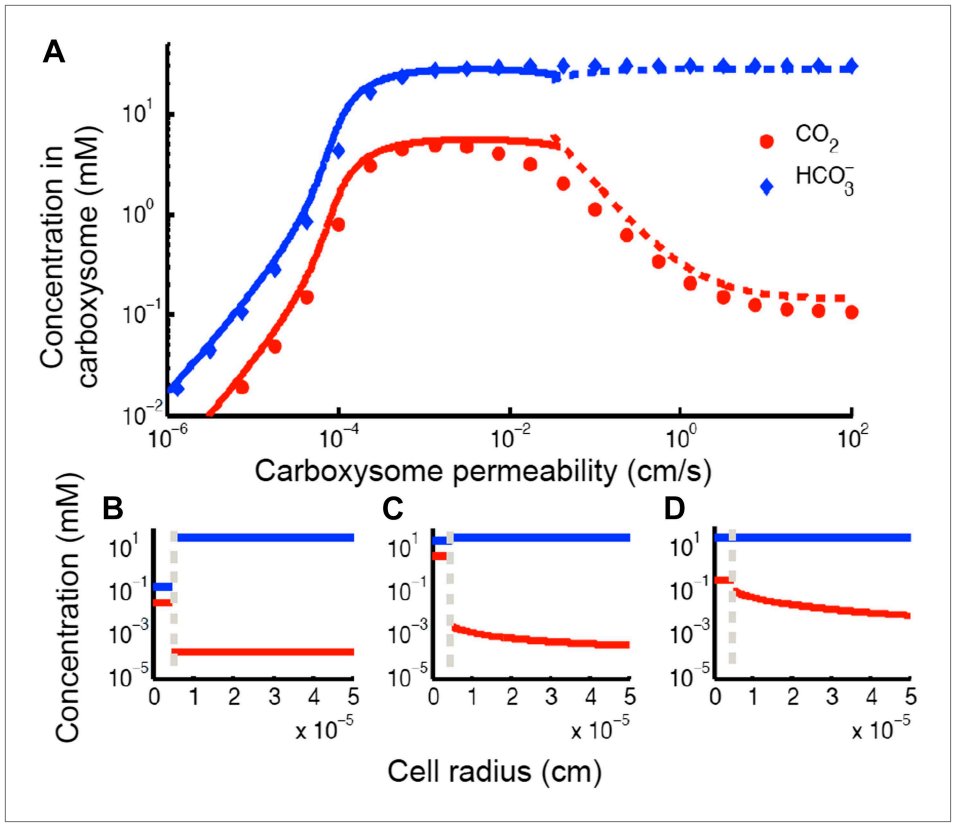

Figure 4. Concentration of CO_2 in the carboxysome with varying carboxysome permeability. (**A**) Numerical solution (diamonds and circles) and analytic solutions (carbonic anhydrase unsaturated, solid lines, and saturated, dashed lines) correspond well. On all plots CO_2 (red circle) < HCO_3^- (blue diamond). Concentration in the cell along the radius, *r*, with carboxysome permeability $k_c = 1e^{-5}\frac{cm}{s}$ (**B**), $k_c = 1e^{-3}\frac{cm}{s}$ (**C**), $k_c = 1\frac{cm}{s}$ (**D**). Grey dotted lines in (**B**), (**C**), (**D**) indicate location of the carboxysome shell boundary. The transition from low CO_2 at high permeability (**D**) to maximum CO_2 concentration at optimal permeability (**C**) occurs at $k_c^* = \frac{D}{R_C} = 2\frac{cm}{s}$. At low carboxysome permeability (**B**) HCO_3^- diffusion into the carboxysome is slower than consumption. For all subplots $\alpha = 0\frac{cm}{s}$ and $j_c = 0.7\frac{cm}{s}$. Qualitative results remain the same with varying j_c, increasing α will increase the gradient of CO_2 across the cell as CO_2 is converted to HCO_3^- at the cell membrane.

DOI: 10.7554/eLife.02043.011

If the carboxysome permeability is below optimal, diffusion of HCO_3^- into the carboxysome cannot keep up with consumption from RuBisCO. The existence of an optima requires RuBisCO consumption to be low enough that there is a k_c where the cytosol and carboxysome are partitioned, but HCO_3^- diffusion in can keep up. When such an optima exists, the carboxysome permeability can improve the CO_2 concentration in the carboxysome without any special selectivity between HCO_3^- and CO_2. The location and concentrating power of the optimal regime, is dependent on the size of the cell and the membrane permeabilities to CO_2 and HCO_3^-.

Discussion

Are the fluxes and concentrations reasonable?

While we have solved our model to describe a vast parameters space it is instructive to compare the fluxes and concentrations we find within our optimal parameter space (the green region in ***Figure 2***) to actual numbers. At low external inorganic carbon conditions, internal inorganic carbon pools due to CCM activity are regularly measured as high as $C_i = 30mM$. The inorganic carbon is predominantly in the form of HCO_3^-, and measurements do not distinguish between the cytosol and carboxysome

(**Sultemeyer et al., 1995**; **Price et al., 1998**, **2008**; **Kaplan and Reinhold, 1999**; **Woodger et al., 2005**). In our model, we find that the cytosolic HCO_3^- concentration is 30 mM when $j_c = 0.7\ \frac{cm}{s}$, over a wide range of the carboxysome permeability (indicated as the dashed grey line in **Figure 2**). From **Figure 4** we can also see that the cytosolic HCO_3^- concentration is the dominate form of inorganic carbon in the cell at $j_c = 0.7\ \frac{cm}{s}$. We examine the fate of the HCO_3^- transported into the cell in terms of the HCO_3^- leaking out, CO_2 leaking out, CO_2 fixation or carboxylation, and O_2 fixation or oxygenation (**Table 3**).

For cells grown under low inorganic carbon conditions net HCO_3^- fluxes (transport–leakage) are measured $10^5\ \frac{\text{pmol}}{(\text{mgChl s})}$, with CO_2 net flux being slightly lower but the same order of magnitude (**Badger et al., 1994**; **Whitehead et al., 2014**). High external inorganic carbon conditions produce slightly higher net HCO_3^- rates (**Tchernov et al., 1997**). Assuming chlorophyll per cell volume of around $10^{-11}\frac{\text{mgChl}}{\text{cell}}$ for cells of our size we can convert this into a flux of $10^{-6}\ \frac{pmol}{(cell\,s)}$ (**Keren et al., 2002**, **2004**; **Whitehead et al., 2014**). The net HCO_3^- flux for our model cell is $10^{-5}\ \frac{pmol}{(cell\,s)}$, so we are about an order of magnitude too high. If we choose a HCO_3^- transport value one order of magnitude smaller, we will get net fluxes of the same order of magnitude as the measurements at the cost of slightly lower carboxylation rates and higher oxygenation rates (**Table 4**). This would also mean a lower internal HCO_3^- pool. Alternatively, the same internal HCO_3^- could be reached at a lower flux rate, if the external HCO_3^- is higher. We have chosen a dramatically low external inorganic carbon concentration, where the CCM is known to be up-regulated (**Price et al., 2008**). The general results we present hold until the internal and external concentration are of the same order of magnitude, at which point the CCM is no longer necessary. Since the majority of the HCO_3^- transport is balanced by HCO_3^- leakage, we can find the transport rate needed to sustain a particular internal concentration by the simple formula: $j_c = k_m^H\left(H_{out} - H_{cytosol}\left(R_b\right)\right)/H_{out}$.

While we can compare the net fluxes, we have not found direct experimental evidence for the absolute HCO_3^- uptake rate. To determine whether this HCO_3^- transport rate is reasonable we perform a back of the envelope calculation. Our simulated cell has a flux of 2×10^7molecules/s. Assuming the rate of transport per transporter of $10^3\ \frac{\text{molecules}}{\text{s}}$ and our cell's surface area this

Table 3. Fate of carbon brought into the cell for $j_c = 0.7\,cm/s$ and $k_c = 6\times10^{-3}$ cm/s

	formula	$\frac{pmol}{(cell\ s)}$	% of flux
HCO_3^- transport	$j_c H_{out}$	3.3×10^{-4}	
HCO_3^- leakage	$k_m^H\left(H_{out} - H_{cytosol}\left(R_b\right)\right)$	3.2×10^{-4}	96.6
CO_2 leakage	$k_m^C\left(C_{out} - C_{cytosol}\left(R_b\right)\right)$	10^{-5}	3.1
carboxylation	$\frac{V_{max}C}{C + K_m\left(1+\frac{O}{K_O}\right)}$	9×10^{-7}	0.3
oxygenation	$\frac{V_{max}^O C}{C + K_m^O\left(1+\frac{C}{K_C}\right)}$	3×10^{-9}	0.001

DOI: 10.7554/eLife.02043.012

Table 4. Fate of carbon brought into the cell for $j_c = 0.07 cm/s$ and $k_c = 6 \times 10^{-3}$ cm/s

	formula	$\frac{pmol}{(cell\ s)}$	% of flux
HCO_3^- transport	$j_c H_{out}$	3.3×10^{-5}	
HCO_3^- leakage	$k_m^H \left(H_{out} - H_{cytosol}(R_b)\right)$	3.2×10^{-5}	95.3
CO_2 leakage	$k_m^C \left(C_{out} - C_{cytosol}(R_b)\right)$	9×10^{-7}	2.8
carboxylation	$\frac{V_{max} C}{C + K_m\left(1 + \frac{O}{K_O}\right)}$	6×10^{-7}	1.7
oxygenation	$\frac{V_{max}^O C}{C + K_m^O\left(1 + \frac{C}{K_C}\right)}$	2×10^{-8}	0.07

DOI: 10.7554/eLife.02043.013

requires about $10^3 \frac{\text{transporters}}{\mu m^2}$. This is actually not that far off from the number of ATP synthase complexes on the thylakoid membrane in spinach, $700 \frac{\text{complexes}}{\mu m^2}$ (***Miller and Staehelin, 1979***), although it is still quite high.

According to our calculation only around 1 % of the inorganic carbon transported into the cell is fixed into 3-phosophoglycerate. The conclusion that about 99% of inorganic carbon transported into the cell is lost through leakage challenges the assumption that the 3 ATP and 2 NADPH used during the Calvin-Benson-Bassham cycle is the dominant energy expenditure. If it holds true, then cyanobacteria invest much more energy in inorganic carbon uptake than was previously understood. Even in this highly CO_2 concentrating regime, 5×10^4 2-phosophoglycolate are produced per second. Cyanobacteria have been shown to have multiple pathways for recycling 2-phosophoglycolate (***Hackenberg et al., 2009***). Our system fixes CO_2 at a rate of 0.14 *pg/hr*. Given the volume of our cell, and the fact that between 115–300 fg/μm^3 of carbon are needed to produce a new cyanobacterial cell (***Mahlmann et al., 2008***) we need between 0.1 and 0.3 picograms of carbon per cell. At the higher flux rate (***Table 3***) this means that a cell could replicate every 1–2 hr, so faster than cyanobacteria replicate. The lower flux rate (***Table 4***) would produce fix enough CO_2 for the cell to replicate every 8 to 21 hr, which is similar to the division times of cyanobacteria.

Concentration profiles of CO_2 and HCO_3^- across the cell

At $j_c = 0.7 \frac{cm}{s}$, varying the carboxysome permeability changes how the available inorganic carbon is partitioned between the carboxysome and cytosol, thereby setting the carboxysomal CO_2 concentration as shown in ***Figure 4***. Strikingly, the HCO_3^- concentration is constant across the cytosol. This is because the cell membranes have low permeability to HCO_3^-; thus, the rate of escape is slow and HCO_3^- equilibrates across the cell. A consequence of this flat HCO_3^- profile is that the carboxysome experiences the same HCO_3^- concentration, independent of its position in the cell. This means the incoming inorganic carbon source for the carboxysome system is invariant with the position of the carboxysome in the cell.

In contrast, there is a gradient in CO_2 concentration across the cell when the carboxysome permeability is at or above the optimum (***Figure 4C,D***). The cell membrane is more permeable to CO_2. The gradient means that the CO_2 leakage out of the cell affects the CO_2 leakage out of the carboxysome. Moving the carboxysome close to the cell membrane increases the leakage rate of CO_2 out of the carboxysome. Notably, in *S. elongatus* the carboxysomes are located along the center line of the cell, away from the cell membranes (***Savage et al., 2010***). The spatial profiles of HCO_3^- and CO_2 give no hint as to why the carboxysomes are spaced apart from one another. Since the gradient in HCO_3^- is flat, there is no competition between the carboxysomes for HCO_3^- (the main incoming source of

inorganic carbon). In fact, since the local concentration of CO_2 is higher near a carboxysome, nearby carboxysomes would "feed" each other CO_2. As has been shown, such clumping would reduce the probability of distributing carboxysomes equitably to daughter cells, possibly counteracting any benefit (***Savage et al., 2010***).

The concentration in the carboxysome is basically constant, because the carboxysome is so small that diffusion across it takes very little time. A consequence of this is that the organization of the reactions in the carboxysome does not effect the CO_2 concentration in the carboxysome (***Figure 3—figure supplement 1***). Therefore, the localization of the carbonic anhydrase to the inner carboxysome shell seems to have no effect on the CCM. It has been suggested that diffusion in the carboxysome should be slower, since the carboxysome is packed with RuBisCO. One proposed consequence of slower diffusion in the carboxysome is that it could trap CO_2, making a low carboxysome permeability unnecessary. We have tested this hypothesis (***Figure 2—figure supplement 1***), and find that assuming the diffusion constant one would expect for small molecules in a 60% sucrose solution ($D_c = 10^{-7}\frac{cm^2}{s}$), does reduce the optimal carboxysome permeability. However, for any carboxysome permeability a higher HCO_3^- transport rate is needed to achieve the same carboxsomal CO_2 concentration. So, if the diffusion is slower in the carboxysome it does not aid the CCM. Even at this slower diffusion, the CO_2 concentration across the carboxysome is flat.

Benefit of CO_2 to HCO_3^- conversion: facilitated uptake or scavenging of CO_2

We investigate the effect of CO_2 to HCO_3^- conversion at the thylakoid and cell membranes (combined in the model). Increasing conversion, $\alpha > 0$, can facilitate uptake of CO_2 from outside the cell and scavenge CO_2 escaped from the carboxysome. Facilitated uptake results in saturating both carbonic anhydrase and RuBisCO at a lower level of HCO_3^- transport. Scavenging broadens the range of carboxysome permeability which will effectively separate the inorganic carbon pools in the carboxysome and outside. Scavenging decreases the concentration of CO_2 in the cytosol, so a more permeable carboxysome can still result in a low leakage rate of inorganic carbon out of the cell (more of the inorganic carbon in the cytosol is in the form of HCO_3^- which leaks out less readily). However, neither of these effects is particularly strong in our current range of reaction rates, and cell membrane permeability (***Figure 2—figure supplement 2***).

The relative effects of these two mechanisms depends on the external CO_2 and HCO_3^- concentrations. In saltwater environments the pH is near 8 and HCO_3^- is the predominant inorganic carbon source. While external pH is not explicitly treated in our model, we can account for changes to pH through the external inorganic carbon concentration. To be consistent with oceanic environment, thus far we have shown results for low external inorganic carbon concentrations of $[CO_2]$ = 0.1 μM and $[HCO_3^-]$ = 14.9 μM. The effect of facilitated uptake, under these assumptions, is very small. In freshwater or under conditions of ocean acidification, where the pH could fall to 6 or lower, there can be a much larger proportion of CO_2 (>50%). ***Figure 5*** shows the absolute contribution of HCO_3^- transport, facilitated CO_2 uptake, and CO_2 scavenging for varying proportions of external CO_2. Even though we assume the same velocity of facilitated uptake and HCO_3^- transport ($j_c = \frac{\alpha}{K_\alpha} = 1\frac{cm}{s}$), facilitated uptake contributes less because it is limited by CO_2 diffusion across the membrane. At the same rates of transport the facilitated uptake mechanism only contributes more than active HCO_3^- if the CO_2 concentration is greater than 80% of external inorganic carbon. This is consistent with observations that oceanic cyanobacteria such as Prochlorococcus only seem to possess gene homologs for HCO_3^- transport systems, while other freshwater and estuarine cyanobacteria have gene homologs for both constitutive (NDH-1_4) and inducible (NDH-1_3) CO_2 uptake systems as well as inducible HCO_3^- transport systems (BicA, SbtA, and BCT1) (***Price, 2011***).

Scavenging only contributes significantly to total incoming HCO_3^- when the carboxysome permeability is higher than optimal, ***Figure 5***, and does not contribute significantly below our caculated upper bound of $k_c < 0.02\frac{cm}{s}$. In these ranges for carboxysome permeability, there is very little CO_2 leaking out of the carboxysome into the cytosol, so there is very little CO_2 to scavenge, ***Figure 5***. The effect of scavenging is dependent on the cell membrane permeability to CO_2 and HCO_3^-.

Given that scavenging has no obvious affect on HCO_3^- concentrations, it is reasonable to wonder why this mechanism exists at all. One might assume that scavenging prevents leakage, but if the energy

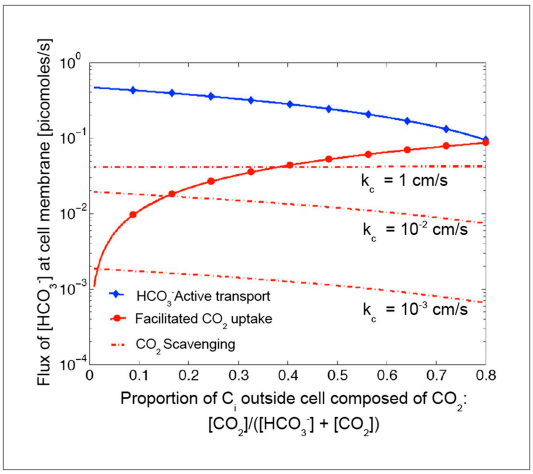

Figure 5. Size of the HCO_3^- flux in one cell from varying sources, as the proportion of CO_2 to HCO_3^- outside the cell changes changes. We show results for three carboxysome permeabilities, k_c, and only the scavenging is effected. Total external inorganic carbon is 15 μM, $j_c = 1\frac{cm}{s}$ and $\frac{\alpha}{K_\alpha} = 1\frac{cm}{s}$. When the carboxysome permeability is larger than optimal, $k_c = 1\frac{cm}{s}$, scavenging can contribute more than facilitated uptake at low external CO_2 concentrations. However, when the carboxysome permeability at or below our geometric bound, $k_c \le 0.02\frac{cm}{s}$, scavenging is negligibly small. Unless there is very little HCO_3^- in the environment, HCO_3^- transport seems to be more efficient than CO_2 facilitated uptake.

DOI: 10.7554/eLife.02043.014

to bring a 'new' HCO_3^- molecule from outside the cell is the same as the energy required to save an 'old' CO_2 molecule from leaking out, there is no obvious advantage of preventing the leakage. It is possible that since the scavenging mechanism is associated with the electron transport chain of the light reactions of photosynthesis scavenging can be ramped up more easily when there is excess light energy. If this were the case, a comparison of $j_c = 1\frac{cm}{s}$ and $\frac{\alpha}{K_\alpha} = 1\frac{cm}{s}$ is deceiving and $\frac{\alpha}{K_\alpha}$ could be much larger. It has been suggested that the cell uses this mechanism as a way to dissipate excess light energy (***Tchernov et al., 1997***, ***2003***).

Cellular organization

The most striking aspect of the CCM is the way that spatial organization is used to increase the efficacy of the reactions. ***Figure 6*** compares the effect of different enzymatic reaction organizations. Concentrating carbonic anhydrase and RuBisCO to a small region in the center of the cell, on a scaffold for example, leads to an order of magnitude increase in the concentration of CO_2. Localizing the carbonic anhydrase to a small volume concentrates it, increasing the maximum reaction rate per volume, V_{ca} and V_{ba}. A larger V_{ba} increases the HCO_3^- concentration at which carbonic anhydrase is saturated allowing the mechanism to take advantage of a larger HCO_3^- flux, j_c. A small increase can be gained from encapsulating the enzymes in a permeable carboxysome shell and another order of magnitude is gained at the optimal permeability. At optimal carboxysome permeability, the CO_2 is effectively partitioned into the carboxysome and conversion can act only as facilitated uptake as shown in ***Figure 5***.

Another advantage of localizing the enzymes in a small region at the center of the cell is separating carbonic anhydrase from the α (CO_2 to HCO_3^-) conversion mechanism, preventing a futile cycle. The futile cycle is most detrimental when the enzymes are distributed throughout the cytosol, and increases the oxygenation error rate by 10% (data not shown). Concentrating the enzymes away from the cell and thylakoid membranes, where conversion happens, removes this effect. With a carboxysome or scaffold the oxygenation rate is almost exactly the same with and without the α conversion mechanism. This is consistent with the previously shown detrimental effect of having active carbonic anhydrase free within the cytosol (***Price and Badger, 1989***). It would be impossible to keep the cytosol completely free from carbonic anhydrase enzyme, so there must be a way of activating it within the carboxysome only. Carbonic anhydrase is inactivated under reducing conditions (***Peña et al., 2010***). Recently it was shown that carboxysomes oxidize after assembly, providing a way to keep carbonic anhydrase inactive until fully enclosed in a carboxysome (***Chen et al., 2013***).

Effects of pH

Cyanobacteria must regulate pH as almost all biochemical reactions are pH sensitive. We do not attempt to model this regulation or potential pH variation within the cell, however pH may be included implicitly in a couple ways. We have already explored the effect of varying external pH, and the effects of pH on carbonic anhydrase. Cytosolic pH would have little direct effect on the CO_2 and HCO_3^- levels since the non-enzymatic interconversion is very slow as previously discussed. The effect of internal pH could also be explored by varying the reaction rate of RuBisCO, which is pH sensitive. Varying the reaction rate of RuBisCO greatly could change the range where a non-specific

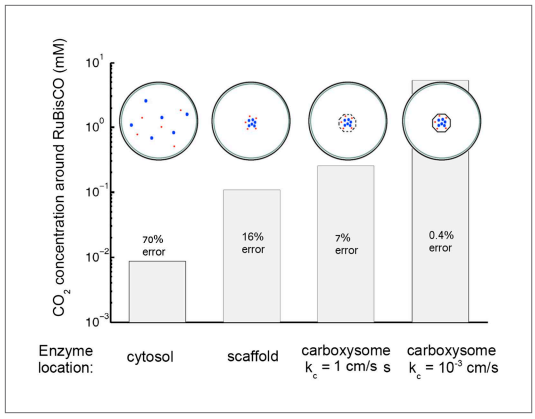

Figure 6. Concentration of CO_2 achieved through various cellular organizations of enzymes, where we have selected the HCO_3^- transport level such that the HCO_3^- concentration in the cytosol is *30 mM*. O_2 concentration is 260 μM. The oxygenation error rates, as a percent of total RuBisCO reactions are indicated on the concentration bars. The cellular organizations investigated are RuBisCO and carbonic anhydrase distributed throughout the entire cytosol, co-localizing RuBisCO and carbonic anhydrase on a scaffold at the center of the cell without a carboxysome shell, RuBisCO and carbonic anhydrase encapsulated in a carboxysome with high permeability at the center of the cell, and RuBisCO and carbonic anhydrase encapsulated in a carboxysome with optimal permeability at the center of the cell.

DOI: 10.7554/eLife.02043.015

carboxysome permeability can increase the concentration of CO_2 in the carboxysome. It would be unexpected that the RuBisCO rate be much faster than we assume, as we have assumed a rate on the high end. A lower RuBisCO rate would increase the range of effective carboxysome permeabilities. As previously mentioned it has been hypothesized that the CO_2 facilitated uptake mechanism functions by creating local alkaline pockets. Diffusion of hydrogen ions across the cell would be very fast, so it could be very difficult to to maintain local alkalinity. Whether such pH gradients are possible, is certainly a subject of future interest.

Conclusions

We have described and analyzed a model for the CO_2 concentrating mechanism in cyanobacteria. There exists a broad range of HCO_3^- transport and carboxysome permeability values which result in effective CO_2 concentration in the carboxysome. This effective concentration parameter space is defined by CO_2 levels high enough to saturate RuBisCO and produce a favorable ratio of carboxylation to oxygenation reactions, but not so high as to saturate carbonic anhydrase (after which increasing HCO_3^- transport will not increase the CO_2 concentration). An optimal, non-specific carboxysome permeability exists, where HCO_3^- diffusion into the carboxysome is not substantially inhibited, but CO_2 leakage is minimal. HCO_3^- concentrations across the cell are flat and are predominately set by the transport rate in, and leakage out. We quantitatively compare the transport rates and concentrations we predict in our optimal parameter space, and find them to be in good agreement with experiment. We also comment on the effects of external pH on CO_2 versus HCO_3^- uptake mechanisms. Finally we describe the cumulative benefits of co-localization, encapsulation, and optimal carboxysome permeability on the CCM.

Further comparison of this model to experimental flux measurements, especially to determine the quantitative contributions of different transporters under different physiological conditions would be very interesting. Current solutions are for steady state at constant external concentration, but most gas exchange measurements, by necessity, measure the fluxes as the inorganic carbon is depleted in the media. The model could be modified to solve the time dependent problem with varying external inorganic carbon. As of yet the carboxysome permeability has not been measured directly, and it would be quite interesting to see how close it is to our 'optimal' prediction.

Acknowledgements

We thank Colleen Cavanaugh, Jeremy Gunarawenda and Pam Silver for important conversations. This research was supported by the National Science Foundation through the Harvard Materials Research Science and Engineering Center (DMR-0820484) and the Division of Mathematical Sciences (DMS-0907985). MPB is an Investigator of the Simons Foundation.

Additional information

Funding

Funder	Grant reference number	Author
NSF Harvard Materials Research Science and Engineering Center	DMR-0820484	Niall M Mangan, Michael P Brenner

Funder	Grant reference number	Author
NSF Division of Mathematical Sciences	DMS-0907985	Niall M Mangan, Michael P Brenner
National Institute of General Medical Sciences	Grant GM068763 for National Centers of Systems Biology	Niall M Mangan, Michael P Brenner

The funders had no role in study design, data collection and interpretation, or the decision to submit the work for publication.

Author contributions

NMM, Performed calculations, Conception and design, Analysis and interpretation of data, Drafting or revising the article; MPB, Oversaw and mentored research, Conception and design, Drafting or revising the article

Additional files

Supplementary file

• Supplementary file 1. Mathematical derivation appendix. Mathematical derivations of analytic solutions for a spherical cell with reactions organized in a variety of ways. We present analytic solutions for the concentration of CO_2 and HCO_3^- a carboxysome located at the center of the cell. We derive analytic solutions assuming a number of different cases for the enzymatic rates in the carboxysome: RuBisCO reaction rate negligible with carbonic anhydrase saturated and unsaturated, RuBisCO reaction rate non-negligible with carbonic anhydrase unsaturated. Additionally we derive analytic solutions for the enzymatic reactions throughout the cell and localized to a scaffold without a carboxysome shell.
DOI: 10.7554/eLife.02043.016

References

Agapakis CM, Boyle PM, Silver PA. 2012. Natural strategies for the spatial optimization of metabolism in synthetic biology. *Nature Chemical Biology* **8**:527–535. doi: 10.1038/nchembio.975.

Allen MM. 1984. Cyanobacterial cell inclusions. *Annual Review of Microbiology* **38**:1–25. doi: 10.1146/annurev.mi.38.100184.000245.

Badger MR, Palmqvist K, Yu JW. 1994. Measurement of CO_2 and HCO_3^- fluxes in cyanobacteria and microalgae during steady-state photosynthesis. *Physiologia Plantarium* **90**:529–536. doi: 10.1111/j.1399-3054.1994.tb08811.x.

Badger MR, Price GD. 2003. CO_2 concentrating mechanisms in cyanobacteria: molecular components and their diversity and evolution. *Journal of Experimental Botany* **54**:609–622. doi: 10.1093/jxb/erg076.

Cannon GC, Bradburne CE, Aldrich HC, Baker SH, Heinhorst S, Shively JM. 2001. Microcompartments in prokaryotes: carboxysomes and related polyhedra. *Applied and Environmental Microbiology* **67**:5351–5361. doi: 10.1128/AEM.67.12.5351-5361.2001.

Cannon GC, English R, Shively JM. 1991. In situ assay of ribulose-1,5-bisphosphate carboxylase/oxygenase in *Thiobacillus neapolitanus*. *Journal of Bacteriology* **173**:1565–1568.

Chen AH, Robinson-Mosher A, Savage DF, Silver PA, Polka JK. 2013. The bacterial carbon-fixing organelle is formed by shell envelopment of preassembled cargo. *PLOS ONE* **8**:e76127. doi: 10.1371/journal.pone.0076127.

Cheng S, Liu Y, Crowley CS, Yeates TO, Bobik TA. 2008. Bacterial microcompartments: their properties and paradoxes. *Bioessays: news and Reviews in Molecular, Cellular and Developmental Biology* **30**:1084–1095. doi: 10.1002/bies.20830.

Cot S, So AK, Espie GS. 2008. A multiprotein bicarbonate dehydration complex essential to carboxysome function in cyanobacteria. *Journal of Bacteriology* **190**:936–945. doi: 10.1128/JB.01283-07.

DeVoe H, Kistiakowsky GB. 1961. The enzymatic kinetics of carbonic anhydrase from bovine and human erythrocytes. *Journal of the American Chemical Society* **83**:274–280. doi: 10.1021/ja01463a004.

Dou Z, Heinhorst S, Williams EB, Murin CD, Shively JM. 2008. CO_2 fixation kinetics of *Halothiobacilus neapolitanus* mutant carboxysomes lacking carbonic anhydrase suggest the shell acts as a diffusional barrier for CO_2. *The Journal of Biological Chemistry* **283**:10377–10384. doi: 10.1074/jbc.M709285200.

Ducat D, Silver P. 2012. Improving carbon fixation pathways. *Current Opinion in Chemical Biology* **16**:337–344. doi: 10.1016/j.cbpa.2012.05.002.

Frank S, Lawrence AD, Prentice MB, Warren MJ. 2013. Bacterial microcompartments moving into a synthetic biology world. *Journal of Biotechnology* **163**:273–279. doi: 10.1016/j.jbiotec.2012.09.002.

Fridlyand L, Kaplan A, Reinhold L. 1996. Quantitative evaluation of the role of a putative CO_2-scavenging entity in the cyanobacterial CO_2-concentrating mechanism. *Bio Systems* **37**:229–238. doi: 10.1016/0303-2647(95)01561-2.

Gutknecht J, Bisson MA, Tosteson FC. 1977. Diffusion of carbon dioxide through lipid bilayer membranes: effects of carbonic anyhdrase, bicarbonate, and unstirred layers. *The Journal of General Physiology* **69**:779–794. doi: 10.1085/jgp.69.6.779.

Hackenberg C, Engelhardt A, Matthijs HCP, Wittink F, Bauwe H, Kaplan A, Hagemann M. 2009. Photorespiratory 2-phosphoglycolate metabolism and photoreduciton of O_2 cooperate in high-light acclimation of *Synechocystis* sp. strain PCC 6803. *Planta* **230**:625–637. doi: 10.1007/s00425-009-0972-9.

Heinhorst S, Williams EB, Cai R, Murin CD, Shively JM, Cannon GC. 2006. Characterization of the carboxysomal carbonic anhydrase CsoSCA from *Halothiobacillus neapolitanus*. *Journal of Bacteriology* **188**:8087–8094. doi: 10.1128/JB.00990-06.

Jordan DB, Ogren WL. 1981. Species variation in the specificity of ribulose bisphosphate carboxylase/oxygenase. *Nature* **291**:513–515. doi: 10.1038/291513a0.

Kaplan A, Reinhold L. 1999. CO_2 concentrating mechanisms in photosynthetic microorganisms. *Annual Review of Plant Physiology and Plant Molecular Biology* **50**:539–570. doi: 10.1146/annurev.arplant.50.1.539.

Keren N, Aurora R, Pakrasi HB. 2004. Critical roles of bacterioferritins in iron storage and proliferation of cyanobacteria. *Plant Physiology* **135**:1666–1673. doi: 10.1104/pp.104.042770.

Keren N, Kidd MJ, Penner-Hahn JE, Pakrasi HB. 2002. A light-dependent mechanism for massive accumulation of manganese in the photosynthetic bacterium *Synechocystis* sp. PCC 6803. *Biochemistry* **41**:15085–15092. doi: 10.1021/bi026892s.

Long BM, Badger MR, Whitney SM, Price GD. 2008. Analysis of carboxysomes from *Synechococcus* PCC7942 reveals multiple RuBisCO complexes with carboxysomal proteins CcmM and CcaA. *The Journal of Biological Chemistry* **292**:29323–29335. doi: 10.1074/jbc.M703896200.

Maeda S, Badger MR, Price GD. 2002. Novel gene products associated with NdhD3/D4-containing NDH-1 complexes are involved in photosynthetic CO_2 hydration in the cyanobacterium, *Synechococcus* sp. strain PCC7942. *Molecular Microbiology* **43**:425–435. doi: 10.1046/j.1365-2958.2002.02753.x.

Mahlmann DM, Jahnke J, Loosen P. 2008. Rapid determination of the dry weight of single living cyanobacterial cells using the Mach-Zehnder double-beam interference microscop. *European Journal of Phyology* **43**:355–364. doi: 10.1080/09670260802168625.

Mayo WP, Elrifi IR, Turpin DH. 1989. The relationship between ribulose bisphosphate concentration, dissolved inorganic carbon (DIC) transport and DIC-limited photosynthesis in cyanobacterium *Synechococcus leopoliensis* grown at different concentrations of inorganic carbon. *Plant Physiology* **90**:720–727. doi: 10.1104/pp.90.2.720.

Miller KR, Staehelin LA. 1979. Analysis of thylalkoid outer surface. Coupling factor is limited ot unstacked membrane regions. *The Journal of Cell Biology* **68**:30–47. doi: 10.1083/jcb.68.1.30.

Missner A, Kügler P, Saparov SM, Sommer K, Mathai JC, Zeidel ML, Pohl P. 2008. Carbon dioxide transport through membranes. *The Journal of Biological Chemistry* **283**:25340–25347. doi: 10.1074/jbc.M800096200.

Omata T, Price GD, Badger MR, Okamura M, Gohta S, Ogawa T. 1999. Identification of an ATP-binding cassette transporter involved in bicarbonate uptake in the cyanobacterium *Synechococcus* sp strain PCC7942. *Proceedings of the National Academy of Sciences of the United States of America* **96**:13571–13576. doi: 10.1073/pnas.96.23.13571.

Papapostolou D, Howorka S. 2009. Engineering and exploiting protein assemblies in synthetic biology. *Molecular Biosystems* **5**:723–732. doi: 10.1039/b902440a.

Peña KL, Castel SE, de Araujo C, Espie GS, Kimber MS. 2010. Structural basis of the oxidative activation of carboxysomal γ-carbonic anhydrase, CcmM. *Proceedings of the National Academy of Sciences of the United States of America* **107**:2455–2460.

Price G. 2011. Inorganic carbon transporters of the cyanobacterial CO_2 concentrating mechanism. *Photosynthesis Research* **109**:47–57. doi: 10.1007/s11120-010-9608-y.

Price G, Badger MR. 1989. Expression of human carbonic anhydrase in the cyanobacterium *Synechococcus* PCC7942 creates a high CO_2-requiring phenotype. *Plant Physiology* **91**:505–513. doi: 10.1104/pp.91.2.505.

Price GD, Badger MR, Woodger FJ, Long BM. 2007. Advances in understanding the cyanobacterial CO_2-concentrating-mechanism (CCM): functional components, C_i transporters, diversity, genetic regulation and prospects for engineering into plants. *Journal of Experimental Botany* **58**:1441–1461. doi: 10.1093/jxb/erm112.

Price GD, Badger MR, Woodger FJ, Long BM. 2008. Advances in understanding the cyanobacterial CO_2-concentrating-mechanism (ccm): functional components, C_i transporters, diversity, genetic regulation and prospects for engineering into plants. *Journal of Experimental Botany* **59**:1441–1461. doi: 10.1093/jxb/erm112.

Price GD, Sultemeyer D, Klughammer B, Ludwig M, Badger MR. 1998. The functioning of the CO_2 concentrating mechanism in several cyanobacterial strains: a review of general physiological characteristics, genes, proteins, and recent advances. *Canadian Journal of Botany* **76**:973–1001. doi: 10.1139/b98-081.

Price GD, Woodger FJ, Badger MR, Howitt SM, Tucker L. 2004. Identification of a SulP-type bicarbonate transporter in marine cyanobacteria. *Proceedings of the National Academy of Sciences of the United States of America* **101**:18228–18233. doi: 10.1073/pnas.0405211101.

Reinhold L, Kosloff R, Kaplan A. 1991. A model for inorganic carbon fluxes and photosynthesis in cyanobacterial carboxysomes. *Canadian Journal of Botany* **69**:984–988. doi: 10.1139/b91-126.

Reinhold L, Zviman M, Kaplan A. 1989. A quantitative model for inorganic carbon fluxes and photosynthesis in cyanobacterial carboxysomes. *Plant Physiology and Biochemistry: PPB* **27**:945–954.

Rosgaard L, de Porcellinis adn JH, Jacobsen AJ, Frigaard NU, Sakuragi Y. 2012. Bioengineering of carbon fixation, biofuels, and biochemcials in cyanobacteria and plants. *Journal of Biotechnology* **162**:137–147. doi: 10.1016/j.jbiotec.2012.05.006.

Savage DF, Alfonso B, Chen A, Silver PA. 2010. Spatially ordered dynamics of the bacterial carbon fixation machinery. *Science* **327**:1258–1261. doi: 10.1126/science.1186090.

Savir Y, Noor E, Milo R, Tlusty T. 2010. Cross-species analysis traces adaptation of RuBisCO toward optimality in a low-dimensional landscape. *Proceedings of the National Academy of Sciences of the United States of America* **107**:3475–3480. doi: 10.1073/pnas.0911663107.

Schmid MF, Paredes AM, Khant HA, Soyer F, Aldrich HC, Chiu W, Shively JM. 2006. Structure of *Halothiobacillus neapolitanus* carboxysomes by cryo-electron tomography. *Journal of Molecular Biology* **364**:526–535. doi: 10.1016/j.jmb.2006.09.024.

Shibata M, Ohkawa H, Kaneko T, Fukuzawa H, Tabata S, Kaplan A, Ogawa T. 2001. Distinct constitutive and low-CO_2-induced CO_2 uptake systems in cyanobacteria: genes involved and their phylogenetic relationship with homologous genes in other organisms. *Proceedings of the National Academy of Sciences of the United States of America* **98**:11789–11794. doi: 10.1073/pnas.191258298.

Sultemeyer D, Price GD, Yu JW, Badger MR. 1995. Characterisation of carbon dioxide and bicarbonate transport during steady-state photosynthesis in the marine cyanobacterium *Synechococcus* strain PCC7002. *Planta* **197**:597–607. doi: 10.1007/BF00191566.

Tcherkez GG, Farquhar GD, Andrews TJ. 2006. Despite slow catalysis and confused substrate specificity, all ribulose bisphosphate carboxylases may be nearly optimized. *Proceedings of the National Academy of Sciences of the United States of America* **103**:7246–7251. doi: 10.1073/pnas.0600605103.

Tchernov D, Hassidim M, Luz B, Sukenik A, Reinhold L, Kaplan A. 1997. Sustained net CO_2 evolution during photosynthesis by marin microorganisms. *Current Biology* **7**:723–728. doi: 10.1016/S0960-9822(06)00330-7.

Tchernov D, Silverman J, Luz B, Reinhold L, Kaplan A. 2003. Massive light-dependent cycling of inorganic carbon between oxygenic photosynthetic microorganism and their surroundings. *Photosynthesis Research* **77**:95–103. doi: 10.1023/A:1025869600935.

Volokita M, Zenvirth D, Kaplan A, Reinhold L. 1984. Nature of the inorganic carbon species actively taken up by the cyanobacterium *Anabaena variabilis*. *Plant Physiology* **76**:599–602. doi: 10.1104/pp.76.3.599.

Whitehead L, Long BM, Price GD, Badger MR. 2014. Comparing the *in vivo* function of α- and β- carboxysomes in two model cyanobacteria. *Plant Physiology* **165**:398–411. doi: 10.1104/pp.114.237941.

Woodger FJ, Badger MR, Price GD. 2005. Sensing of inorganic carbon limitation in *Synechococcus* PCC7942 is correlated with the size of the internal inorganic carbon pool and involves oxygen. *Plant Physioogyl* **139**:1959–1969. doi: 10.1104/pp.105.069146.

Yeates TO, Kerfeld CA, Heinhorst CAK, Cannon GC, Shively JM. 2008. Protein-based organelles in bacteria: carboxysomes and related microcompartments. *Nature Reviews Microbiology* **6**:681–691. doi: 10.1038/nrmicro1913.

Yeates TO, Tsai TY, Tanaka S, Sawaya MR, Kerfeld CA. 2007. Self-assembly in the carboxysome: a viral capsid-like protein shell in bacterial cells. *Biochemical Society Transactions* **35**:508–511. doi: 10.1042/BST0350508.